

## Preparation of Activated Carbon Monolith Electrodes from Sugarcane Bagasse by Physical and Physical-chemical Activation Process for Supercapacitor Application

E. Taer<sup>1\*</sup>, Iwantono<sup>1</sup>, S. T. Manik<sup>1</sup>, R. Taslim<sup>1</sup>, D. Dahlan<sup>2</sup>, M. Deraman<sup>3</sup>

<sup>1</sup>Department of Physics, University of Riau, 28293 Simpang Baru, Riau, Indonesia

<sup>2</sup>Material Physics laboratory, Department of Physics, Andalas University, Limau Manis Padang 25163, West Sumatra, Indonesia

<sup>3</sup>School of Applied Physics, Faculty of Science and Technology, Universiti Kebangsaan Malaysia, 43600 Bangi, Selangor, Malaysia

\*Corresponding author e-mail: erman\_taer@yahoo.com

**Keywords:** Supercapacitor, Activated carbon monolith, Sugarcane bagasse.

**Abstract:** Binderless activated carbon monoliths (ACMs) for supercapacitor electrodes were prepared from sugarcane bagasse by two different methods of physical and combination of physical-chemical activation process. The CO<sub>2</sub> gas was used as physical activation agent and 0.3 M KOH was chosen as chemical activation agent. The ACMs were tested as electrodes in two-electrode systems of the coin tape cell supercapacitor that consists of stainless steel as current collectors and 1 M H<sub>2</sub>SO<sub>4</sub> as an electrolyte. The improving of resistive, capacitive and energy properties of combination of physical-chemical ACMs electrodes were shown by an impedance spectroscopy, a cyclic voltammetry and a galvanostatic charge-discharge method. The improving of resistive, capacitive and energy properties as high as 1 to 0.6 Ω, 141 to 178 F g<sup>-1</sup>, 3.83 to 4.72 W h kg<sup>-1</sup>, respectively. The X-ray diffraction analysis and field emission scanning electron microscope were performed to characterize the crystallite and morphology characteristics. The results showed that the combination of physical-chemical activation process have given a good improving in performance of the bagasse based ACMs electrodes in supercapacitor application.

### Introduction

A supercapacitor also known as an electrochemical double layer capacitor (EDLC) is energy storage device, similar to conventional capacitors, batteries, and fuel cell [1]. The EDLC commonly use a carbon material as an electrode. Energy storage in EDLC occurs because of the formation of ions pair in the electrolyte and electrons in the carbon material at the interface between the electrolyte and carbon electrodes [2]. Activated carbon in a decade has been widely used as supercapacitor electrodes because their some superiority properties, such as high surface area, abundant availability, chemically stable and relatively low cost. Based on the low price consideration, biomass material is very interesting to be used as a source material for the manufacture of activated carbon [3]. Sugarcane bagasse (SB) is the biomass materials commonly used in the production of activated carbon by chemical activation method with ZnCl<sub>2</sub> as activation agent [4,5]. The SB can also be used as scaffold for producing activated carbon monolith electrodes [6]. The specific capacitance ( $C_{sp}$ ) and specific energy are in range 140 to 300 F g<sup>-1</sup> and 10 to 30 Wh kg<sup>-1</sup>, respectively. In this study, it will be demonstrated a production of activated carbon monolith electrode from SB with a combination of physical and chemical activation. Combination of physics and chemical activation on carbon materials from SB has shown significant improvements in the resistive and capacitive properties of the supercapacitor cell.

### Experimental Procedure

Two different ACMs electrodes were prepared from the SB using our previously reported method [7]. The first electrode was prepared by physical activation process using CO<sub>2</sub> gas that followed our previous study [8] and labeled as ACM1. The second one prepared by combination of physical and chemical activation process and labeled as ACM2. The chemical activation was



performed by using 0.3 M KOH, all procedure in production of ACM2 has been reported [7]. The symmetrical supercapacitor cells were fabricated to study the capacitive properties of the ACMs to be used as electrodes as our previous reported [8].

Surface morphology and structure were evaluated in the present study. The morphological structures of the ACM were elucidated on a FESEM (Supra PV 55 model). The structure of the ACM was elucidated by XRD. The XRD patterns were obtained on a Bruker AXS D8 advance diffractometer that employed  $\text{CuK}_\alpha$  radiation with a  $2\theta$  range of 0 to  $60^\circ$ . The performance of the supercapacitor cells was studied by a galvanostatic charge-discharge (GCD), EIS and cyclic voltammetry (CV) using a Solatron 1286 electrochemical interface. The  $C_{sp}$  value of the cell for each measurement method was determined using standard formulas [7].

## Results and Discussion

Fig. 1(a) shows the FESEM micrographs for the samples with two different of activation method, ACM1 and ACM2. These micrographs clearly show that ACM2 is more porous than ACM1, which has evenly distributed pores with high density. This difference further supports the hypothesis that activation method instrumental in the formation of the pore network or porous matrix in the ACM derived from SB.

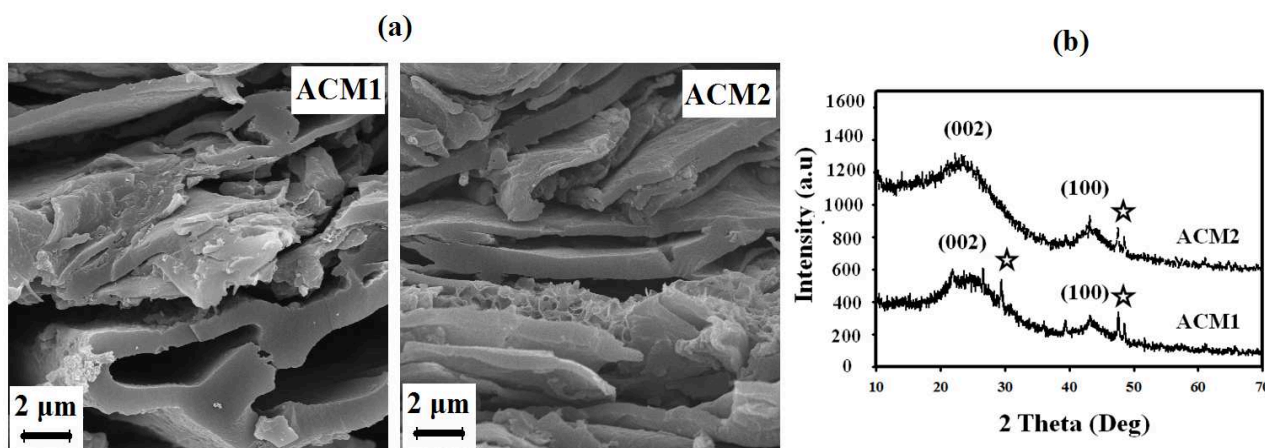


**Figure 1.** (a): SEM micrograph of ACMs electrodes (b): X-ray diffractogram of ACMs electrodes.

Fig. 1(b) shows the XRD patterns of the ACM1 and ACM2 electrodes. Broad peaks corresponding to (002) and (100) planes of the carbon structure appear in both XRD patterns between  $15$  and  $35^\circ$ . The sharp peaks that appear on the broad peaks labeled with the star are due to the presence of  $\text{SiO}_2$  in the electrode. The different technique in activation resulted in the peaks corresponding to  $2\theta$  at  $23.981$  and  $44.520^\circ$  for ACM-1 shifting to  $24.423$  and  $45.520^\circ$  for ACM2, respectively. This shift is due to the decrease in the interlayer spacing,  $d_{002}$ , from  $0.371$  to  $0.364$  nm and in  $d_{100}$  from  $0.203$  to  $0.199$  nm. Furthermore, the values of  $L_c$  and  $L_a$  calculated from these peaks also changed with addition of chemical activation process. The values of  $L_c$  and  $L_a$  were  $1.147$  and  $2.286$  nm for ACM1 and  $0.856$  and  $2.168$  nm for ACM2, respectively, indicating a decrease in the dimension of the graphitic crystallites.

Fig. 2(a) presents the EIS spectra in the form of Nyquist plots for both of the supercapacitor cells using the ACM1 and ACM2 electrodes. In this figure,  $R_s$  represents the resistance of the electrolyte and interfacial resistance between the current collector and electrodes.  $R_p$  is the intrinsic resistance of the electrodes, and  $R_f$  is the equivalent series resistance of the distributed pore resistance in the electrodes. The values of  $R_s$ ,  $R_p$  and  $R_f$  of both cells ACM1 and ACM2, estimated from Fig. 2(a), are listed in Table 1. From the magnified EIS spectra of the cells (Fig. 2(a)-inset), it can be seen that both sample show a semicircular pattern in the higher frequency region, combination of chemical and physical activation process and indicate the decrease in internal resistance of the porous electrode. The  $C_{sp}$  values of the cell are also listed in Table 1.

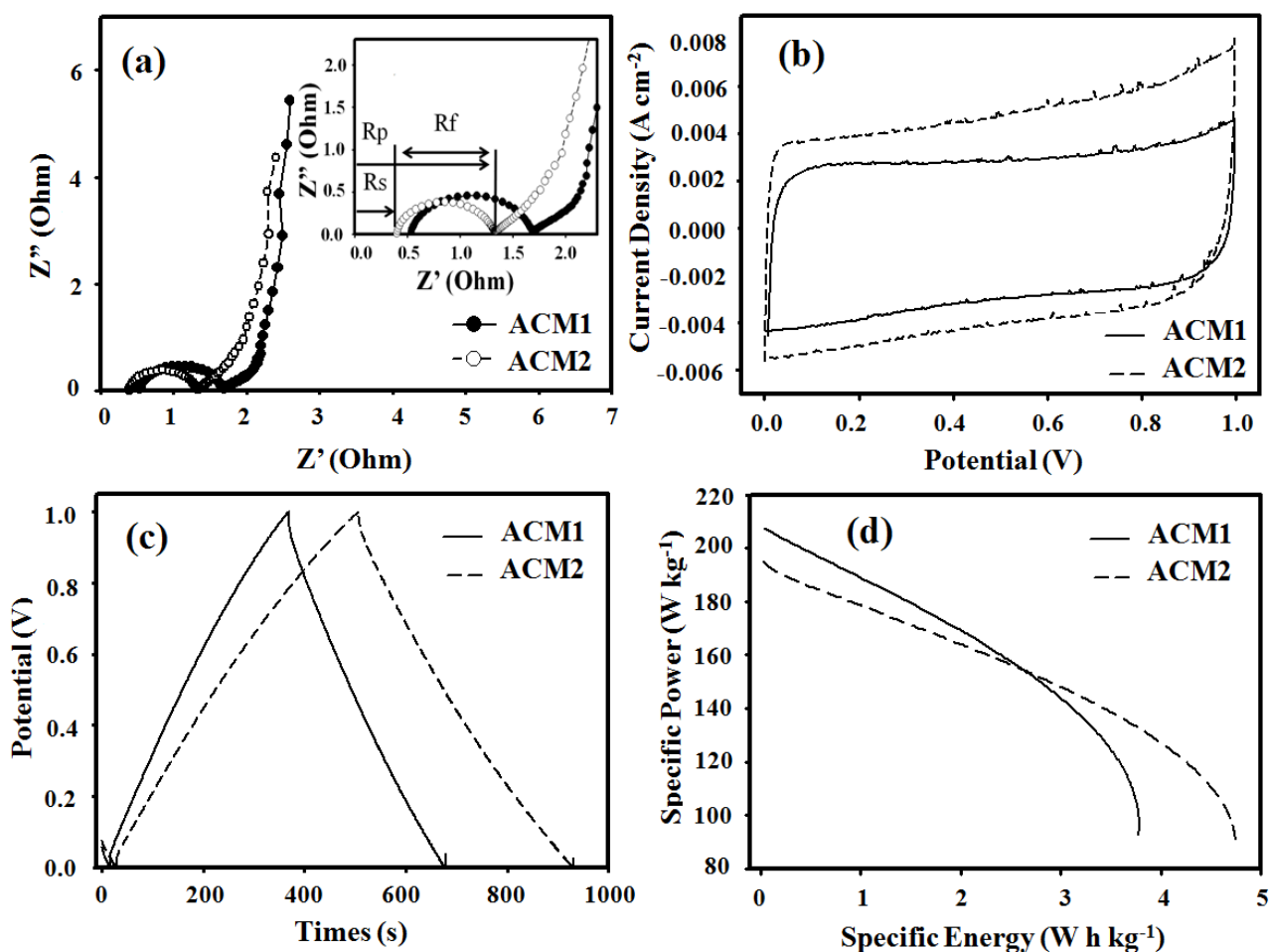


**Figure 2.** (a): Nyquist plot from EIS data, (b): The cyclic voltammogram data, (c): The charge and discharge curve data at constant current and (d): Ragone plot data for supercapacitor cells with electrode ACM1 and ACM2.

The CV of the supercapacitor cells based on ACM1 and ACM2 electrodes are shown in Fig. 2(b) for the potential window from 0 to 1 V with a scan rate of  $1 \text{ mV s}^{-1}$ . Both cells had similar rectangular-like shapes in the potential range of investigation. A combination of activation process led to an increase in the current values of the voltammograms. This is a consequence of the increase porosity properties with the addition of chemical activation process and in the accessibility of electrolytes to the porous matrix of electrodes and  $C_{sp}$  values of the cell are listed in Table 1.

The GCD studies of the supercapacitor cell were performed between cell voltages of 0.01 and 1.0 V at discharge current densities of  $10 \text{ mA cm}^{-2}$ , as shown in Fig. 2(c). Both of the charge-discharge curves had a similar shape, which is a typical pattern for carbon electrode-based cells with capacitive behavior [9]. The supercapacitors based on ACM2 had longer discharge times than the ACM1-based cells. The  $C_{sp}$  values of the cell are also listed in Table 1.

The Ragone plots for the supercapacitor cells with ACM1 and ACM2 electrodes are shown in Fig. 2(d). The energy and power relationship of this plot was calculated by applying the standard formulas [7] from the discharge curves at a current density of  $10 \text{ mA cm}^{-2}$  (Fig. 2(c)). A gradual decrease in specific power was observed with increasing specific energy for the cells employing the both ACM electrodes. These results fall within the typical range of specific energy and specific power density for supercapacitors [10].

For comparison the results obtained in this study, our result from cell with ACM2 electrode seem to be within the range of the reported values [5-7], indicating that combination of chemical and physical activation process in modifying the surface of the ACM electrode could be considered a satisfactory method for obtaining efficient supercapacitor electrodes because this method is lower

concentration of chemical activation agent has been promoted the existing of more porous electrode materials and lower cost compared to other methods.

**Table 1.** Resistances, specific capacitances, maximum energy and power of the supercapacitor cells.

Samples	$R_s$ ( $\Omega$ )	$R_p$ ( $\Omega$ )	$R_f$ ( $\Omega$ )	$C_{sp}$ ( $F g^{-1}$ )			$E_{max}$ $W h kg^{-1}$	$P_{max}$ $W kg^{-1}$
				EIS	CDC	CV		
ACM1	0.41	1.59	1.18	146.89	141.79	140.12	3.83	209
ACM2	0.47	1.07	0.60	152.29	178.31	170.72	4.72	193

### Summary

Based on the studies using the EIS, CV and GCD methods, it was consistently found that supercapacitor cells using ACM2 electrodes, electrode were active by combination of chemical and physical agent, exhibited better supercapacitive performance compared to the cells using the physical activation based monolithic carbon electrodes. It can be concluded that the role low concentration of chemical activation agent is significant towards achieving a 49%, 20% and 21% improvement in the ESR, specific capacitance and specific energy of the supercapacitor cells, respectively.

### Acknowledgments

The authors acknowledge the research grant International Research Collaboration and Scientific Publication 2013, Indonesia and Research University grants (UKM-GUP-2011-216, UKM-DLP-2012-022 and UKM-DLP-2012-023) Malaysia.

### References

- [1] A. Burke: J. Power Sources, 91(2000), 37-50.
- [2] R. Kotz: Electrochim. Acta, 45(2000), 2483-2498.
- [3] C. Peng, X.- bin Yan, R.- tao Wang, J.- wei Lang, Y.- jing Ou and Q.- ji Xue: Electrochim. Acta, 87(2013), 401-408.
- [4] T.E. Rufford, D.H.- Jurcakova, K. Khosla, Z. Zhu and G.Q: Lu. J. Power Sources, 195(2010), 912-918.
- [5] S.W- Jiang, W.X- Zhong, X. Wei, Z. Jin and Z.S- Ping: J. Inorganic Mater, 26(2011), 107-112.
- [6] C.-H. Huang and R.-A. Doong: Microporous and Mesoporous Mater, 147(2012), 47-52.
- [7] R. Farma, M. Deraman, A. Awitdrus, I.A. Talib, E. Taer, N.H. Basri, J.G. Manjunatha, M.M.Ishak, B.N.M. Dollah and S.A. Hashmi: Bioresource Technol, 132(2013), 254-261.
- [8] E. Taer., M. Deraman., I.A. Talib., A. Awitdrus., S.A. Hashmi and A.A. Umar, Int. J. Electrochem. Sci, 6(2011), 3301-3315.
- [9] M. Inagakia., H. Konno and O. Tanaike: J. Power Sources, 195(2010), 7880-7903.
- [10] E. Taer, M. Deraman, I.A. Talib, S.A. Hashmi and A.A. Umar: Electrochim. Acta, 56 (2011), 10217-10222.